ENVIRONMENTAL AUDITING
An Approach for Characterizing Tropospheric Ozone Risk to Forests

WILLIAM E. HOGSETT*
JAMES E. WEBER
DAVID TINGEY
US EPA, Environmental Research Laboratory—Corvallis
200 SW 35th
Corvallis, Oregon 97333, USA

ANDREW HERSTROM
E. HENRY LEE
ManTech Inc
200 SW 35th
Corvallis, Oregon 97333, USA

JOHN A. LAURENCE
Boyce Thompson Institute for Plant Research
Tower Rd
Ithaca, New York 14853, USA

ABSTRACT / The risk tropospheric ozone poses to forests in the United States is dependent on the variation in ozone exposure across the distribution of the forests in question and the various environmental and climate factors predominant in the region. All these factors have a spatial nature, and consequently an approach to characterization of ozone risk is presented that places ozone exposure–response functions for species as seedlings and model-simulated tree and stand responses in a spatial context using a geographical information systems (GIS). The GIS is used to aggregate factors considered important in a risk characterization, including: (1) estimated ozone exposures over forested regions, (2) measures of ozone effects on species' and stand growth, and (3) spatially distributed environmental, genetic, and exposure influences on species' response to ozone. The GIS-based risk characterization provides an estimation of the extent and magnitude of the potential ozone impact on forests. A preliminary risk characterization demonstrating this approach considered only the eastern United States and only the limited empirical data quantifying the effect of ozone exposures on forest tree species as seedlings. The area-weighted response of the annual seedling biomass loss formed the basis for a sensitivity ranking: sensitive—aspen and black cherry (14%–33% biomass loss over 50% of their distribution); moderately sensitive—tulip popular, loblolly pine, eastern white pine, and sugar maple (5%–13% biomass loss); insensitive—Virginia pine and red maple (0%–1% loss). In the future, the GIS-based risk characterization will include process-based model simulations of the three- to 5-year growth response of individual species as large trees with relevant environmental interactions and model simulated response of mixed stands. The interactive nature of GIS provides a tool to explore consequences of the range of climate conditions across a species' distribution, forest management practices, changing ozone precursors, regulatory control strategies, and other factors influencing the spatial distribution of ozone over time as more information becomes available.

Ecological risk assessment has been defined as a process that evaluates the likelihood of adverse effects resulting from exposure to one or more stressors (US EPA 1992a). For a risk to exist, the stressor(s) must have the ability to cause one or more adverse effects and cooccur with or contact an ecological component (e.g., species, population, community, ecosystem) long enough and at sufficient concentrations to cause the identified adverse effect(s).

Assessing the risk to forests from tropospheric ozone requires quantification of the phytotoxic effects of ozone at the appropriate biological level (e.g., individual species, population, or community) under ambient exposure characteristics and the identification of the types of uncertainties associated with these effects. Defining which of these effects are adverse requires knowledge of the extent and magnitude of the effect, exposure characteristics over the appropriate landscape scale (e.g., watershed, region, national), and the consequences of these effects to society. This determination requires input from both science and the public. Although Webster's Dictionary defines ''adverse'' as ''opposed to one's interest or welfare; harmful or detrimental,'' the evaluation process for adverse ozone effects should take into account both societal and ecological values and should recognize that not all effects are equally important. Tingey and others (1990) suggested adverse effects could be classified into one or more of the following categories: (1) economic produc-

KEY WORDS: Ecological risk assessment; GIS; Ozone; Risk characterization; Forests; Trees

*Author to whom correspondence should be addressed.

tion, (2) ecological structure, (3) genetic resources, and (4) cultural values. Within each of these categories there might be a number of measurable adverse effects to forests whose protection would be the goal of a secondary National Ambient Air Quality Standard (NAAQS). The secondary NAAQS sets the permissable level of tropospheric ozone to prevent adverse effects to forests, among other welfare resources.

Suter (1990) describes the activities involved in an ecological risk assessment after the adverse effect(s) or assessment end points are identified. First, the problem is defined. This entails choosing measurement end points for the selected assessment end points and describing the environment and the hazard, which in this case means estimating the magnitude and spatial variation of ozone exposure over forests and the cooccurring relevant environmental conditions. Problem definition is followed by a formal analysis of the measured effects, including integration of the exposure, environment, and effects data to estimate the magnitude and spatial extent of stressor impact.

Forests can be assessed at many biological levels, most of which we do not understand sufficiently to quantify the impact of tropospheric ozone. At the species level, however, in terms of both individuals and populations, we can identify a number of assessment end points. For the purposes of illustrating the GIS-based approach for a risk characterization, we use productivity as the assessment end point. Productivity has social relevance and can be related to the economic value of timber products, recreation, and carbon sequestration. Equally important, productivity can also be related to ecological values through individual species' growth rates and the resulting community species composition and genetic diversity in the loss of sensitive individuals or species. Productivity is measurable through growth or change in biomass at the individual and population levels, which has been shown to be affected directly and indirectly by ozone exposure (Pye 1988, Miller and others 1989). For the assessment end point of productivity, the relevant measurement end point then is a change in growth rates and biomass. A limited amount of data that quantifies growth and biomass changes for seedlings and saplings exposed to tropospheric ozone is currently available; these data were used in our preliminary assessment described in this paper.

For the spatial characterization of ozone impact to forests, a geographical information system (GIS) can be used to integrate both empirical data of growth effects-based exposure–response functions and model simulations of long-term growth effects of ozone exposure with geographical data of the species' distribution, regional ozone exposure, and climate/environmental factors across forested areas. In its simplest form, GIS technology is computerized mapping and map analysis that provides the ability to integrate data from various sources and spatial/temporal scales. Conceptually, data within the GIS exist as layers of spatially coincident digital maps with each map layer representing one particular theme such as species distributions, estimated ozone exposures, or an influencing environmental factor (Figure 1). A geographic context is useful for risk characterization because of the spatial variation of a regional air pollutant such as ozone, as well as the variations in climate and land use that directly influence a tree's ability to absorb and detoxify ozone. The GIS-based risk characterization offers a means to establish a ranking of species' sensitivities based on area-weighted growth response, and a spatial context for the extent and magnitude of ozone's impact on individual forest species.

To illustrate the GIS-based approach, we have used the eastern United States (the conterminous states east of the 100th meridian) as the study area. The eastern United States contains 10 forest types and a substantial number of forest tree species (Eyre 1980) and resource uses. Our example of the risk characterization is based on change in biomass (productivity) of eight tree species as seedlings.

Methods

Assessment Structure

The GIS provides the framework for integrating the several sets of data representing ozone exposure and effects, including: (1) estimated ozone exposure (including precursor emissions, meteorology, landscape features), (2) species distribution, (3) species density, (4) influential environmental factors (biotic and abiotic), and (5) species' exposure–response functions for the selected measurement end point (Figure 1). The data exist at various spatial and temporal resolutions and are taken from the published literature and geographical and land-use data bases. In the GIS, a grid of 20-km-square cells measuring 140 cells north–south by 135 cells east–west (18,900 cells total) was generated and superimposed over the study area. Each cell is considered as a homogenous unit for any given factor, and so each cell contains one value for each of the above-listed data.

In the GIS, the exposure–response function is combined with the geographic data layers (estimated ozone exposure over the region, spatial distribution of each species, and relevant environmental and genotypic data) to generate a data layer that depicts the potential risk of the forest species in a spatial context (Figure 1).

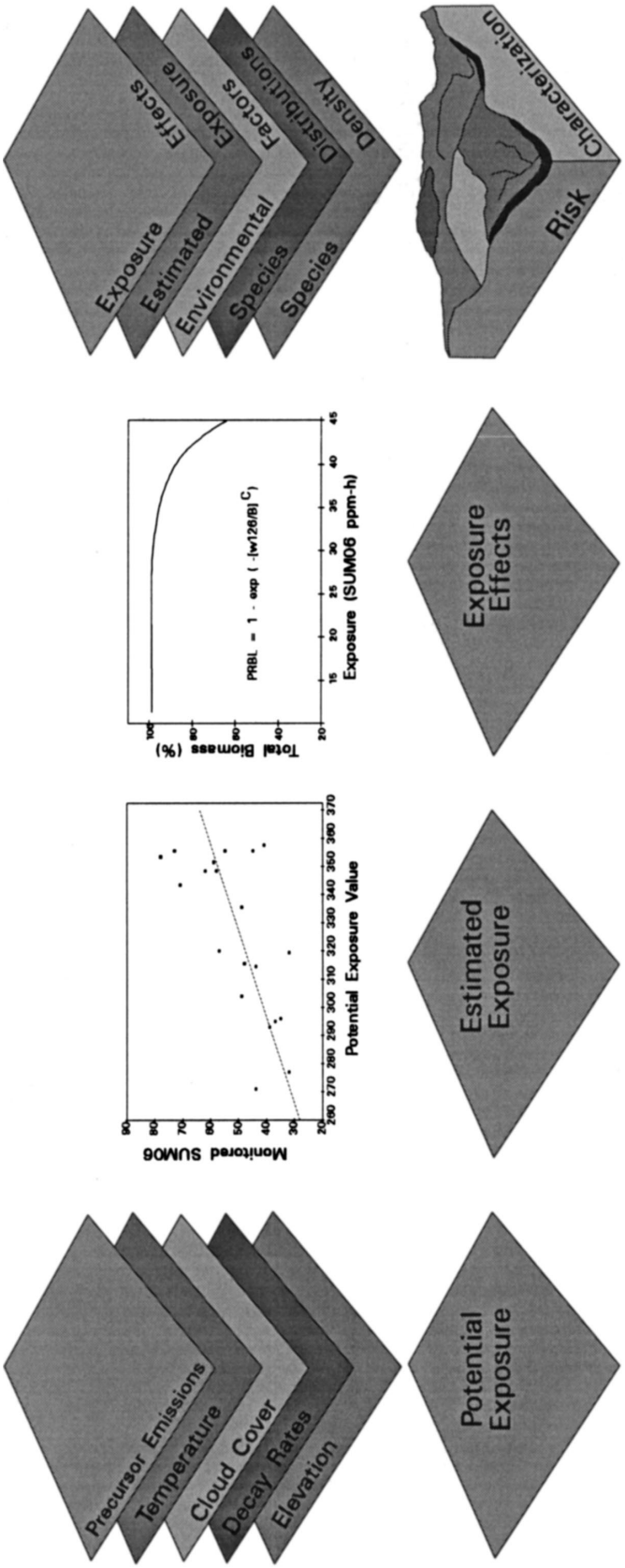

Figure 1. GIS data layers for the components of the risk characterization, including GIS-based estimation of ozone exposure in nonmonitored areas, seedling-based exposure response functions for each species, and the combination of effects, including influential environmental factors, and exposure information within the GIS to generate a new data layer describing risk. Risk is described as a predicted relative annual biomass loss in each 20-km grid over the species' distribution.

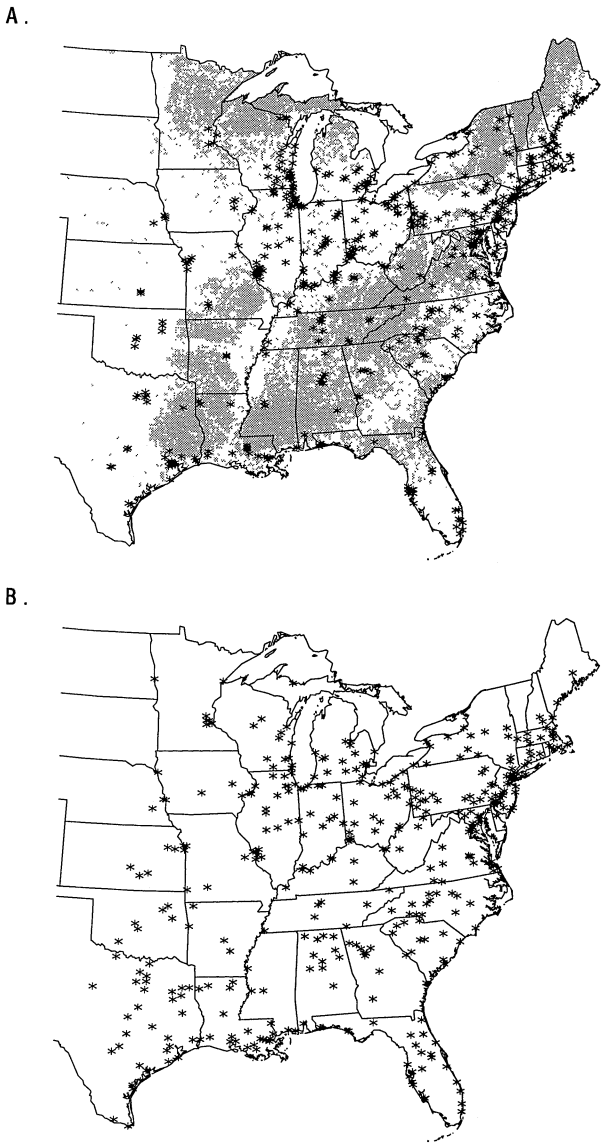

Figure 2. **A:** EPA AIRS ozone monitoring sites (*) across the eastern US comapped with forested areas (shaded). **B:** Location of the 417 largest anthropogenic NO_x emission sources (counties) in the eastern U.S. Asterisks denote the county centroid.

Estimation of Ozone Exposure over Forests

Characterization of ozone exposure has typically involved the use of descriptive statistics to describe ozone behavior at monitored sites within broad geographic regions (Pinkerton and Lefohn 1987, Wolff and others 1987, Logan 1988, Lefohn and Lucier 1991). This approach would be acceptable for assessing ozone risk in forests only if the set of monitored sites were representative of forested areas in the region and if exposures were relatively homogenous throughout these forested areas. However, most monitored ozone sites are located in urban or near-urban areas, and observations suggest that monitored values are representative of rather specific and limited areas rather than broad geographic regions (National Research Council 1991). Nationally, approximately 79% of all ozone monitoring sites are classified as residential, commercial, or industrial (i.e., urban or near-urban); 17% are classified as agricultural; 3% are classified as desert or mobile; and less than 2% are classified as being forested (US EPA 1986). Figure 2A shows how relatively few monitoring sites in the eastern United States exist in forested areas. Because of this situation, tropospheric ozone exposures for most forested areas must be estimated.

We used an ad hoc method based on factors that influence ozone formation and transport to estimate monthly to seasonal ozone concentrations in nonmonitored areas (Hogsett and Herstrom 1991). We have estimated the three-month, 24-h SUM06 exposure value (Lee and others 1988). The SUM06 index cumulates all hourly values equal to or greater than 60 ppb over the maximum three months of the year. Generally, these three months are the major growing period for plants, including June, July, and August or July, August, and September. Such an index reflects the observation that plants are affected to a greater degree by higher concentrations, and the duration of the exposure is important in the biological response (Hogsett and others 1988, Musselmann and others 1994). Our method for estimating seasonal exposure considers more than the distance between urban and near-urban monitored sites, the factor used as the basis for most standard interpolation techniques such as distance weighting (Watson and Phillip 1985) and kriging (Oliver 1990) but which has limitations even for ozone estimations in agricultural areas (Lefohn and others 1987). A GIS is used to generate a surface of ozone exposure potential based on ozone precursor and meteorological factors that influence ozone formation, transport, and attenuation (Figure 3A). We considered several factors to be influential (Table 1): (1) ozone-forming precursors as represented by emissions of anthropogenic NO_x, (2) daily maximum temperature, (3) daily cloud cover, (4) wind direction, (5) elevation, and (6) distance from the emission source (used with estimated decay rate of ozone). The emissions data are from 1985 and the meterological data are year-specific hourly values. The fact that volatile organic carbon (VOC) concentrations (anthropogenic and biogenic), and VOC/NO_x ratios in particular, are important in determining the amount of ozone formed (National Research Council 1991) is recognized. In this estimation, however, NO_x is the only precursor considered since in our analysis it appeared to be limiting. Each of the factors is treated as a matrix

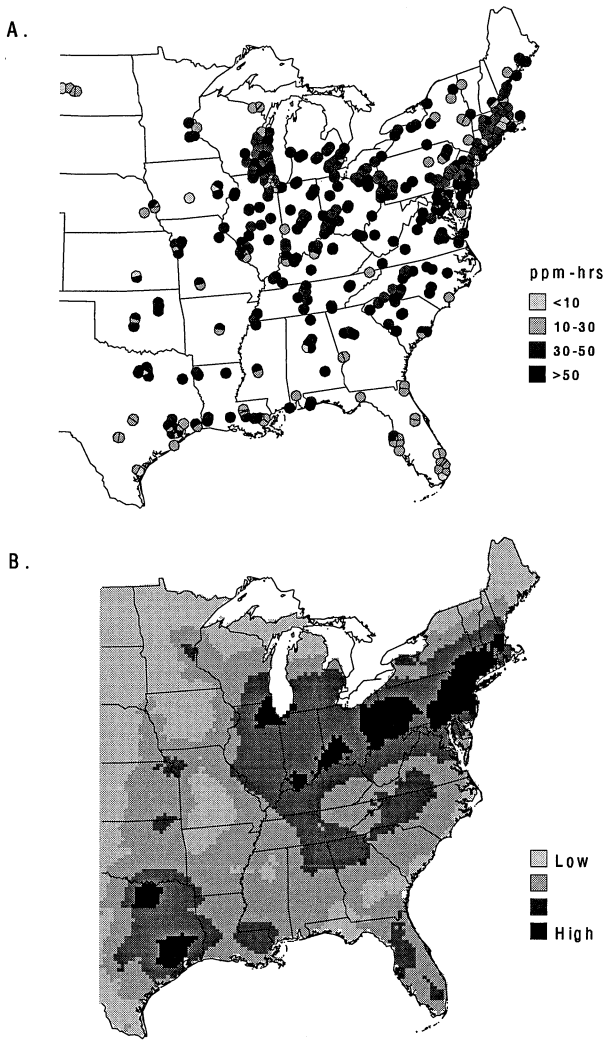

Figure 3. A: 1988 ozone monitoring site locations (294) and calculated three-month, 24-h SUM06 at each site. **B:** Ozone exposure potential surface EPS, generated using factors given in Table 1. Increasing potential for high ozone exposure is indicated with increasing degree of shading.

Table 1. Ozone precursor emissions and meteorological factors used to generate ozone exposure potential surface

Factor	Source	Spatial and temporal scale
1. Anthropogenic NO_x	US EPA (1992a)	Estimates of annual county totals 1985 (tons per year) (assumes equal monthly emission values)
2. Daily wind direction	Earthinfo (1992a)	Hourly values measured at 273 major airports (values interpolated to each 10-km cell using inverse distance squared)
3. Daily cloud cover	Earthinfo (1992a)	Hourly values measured at 273 major airports (values interpolated to each 10-km cell using inverse distance squared)
4. Daily maximum temperature	Earthinfo (1992b)	Daily maximum value measured at 5100 sites (values interpolated to each 10-km cell using inverse distance squared)
5. Elevation	Loveland and others (1991)	Mean elevation resampled to 1-km resolution
6. Distance from emission source	ESRI	Determined by the GIS software

of values or a data layer within the GIS (Figure 1). The 417 largest emitting counties are used as sources, accounting for approximately 70% of the total anthropogenic NO_x emissions in the study area (Figure 2B). Population centers are considered as the origin of all NO_x emissions. Ozone is ''formed'' based on amount of NO_x, temperature, cloud cover, and stagnant air masses and is dispersed from each population center (US Department of Commerce 1992) based on decay rate (distance from emission source) and wind direction. Combined, the layers yield the unitless exposure potential surface (EPS), which consists of a grid of regularly spaced relative values 20 km apart. The density of these exposure potential values is far greater than the density of monitored ozone sites (which can be hundreds of kilometers apart); thus, assuming the surface is a reliable indicator of relative ozone exposure, the ability to capture trends and variation of exposure between monitored sites is theoretically improved.

The relationship between the maximum three-month, 24-h SUM06 (Lee and others 1988) ozone values from each monitored site (Figure 3A) and the corresponding exposure potential (PES) values (Figure 3B) is used to translate the unitless PES values at each 10-km cell into a SUM06 estimate. This is accomplished by calculating the ratio of the monitored SUM06 exposure to the PES value at every monitored site and interpolating these ratios across the study area such that each cell receives an estimate of the SUM06/PES ratio. The interpolated SUM06/PES ratio at each cell is multiplied by the PES value for that cell to produce an estimate of SUM06 exposure for that cell. At every monitored site the SUM06/PES ratio times the PES

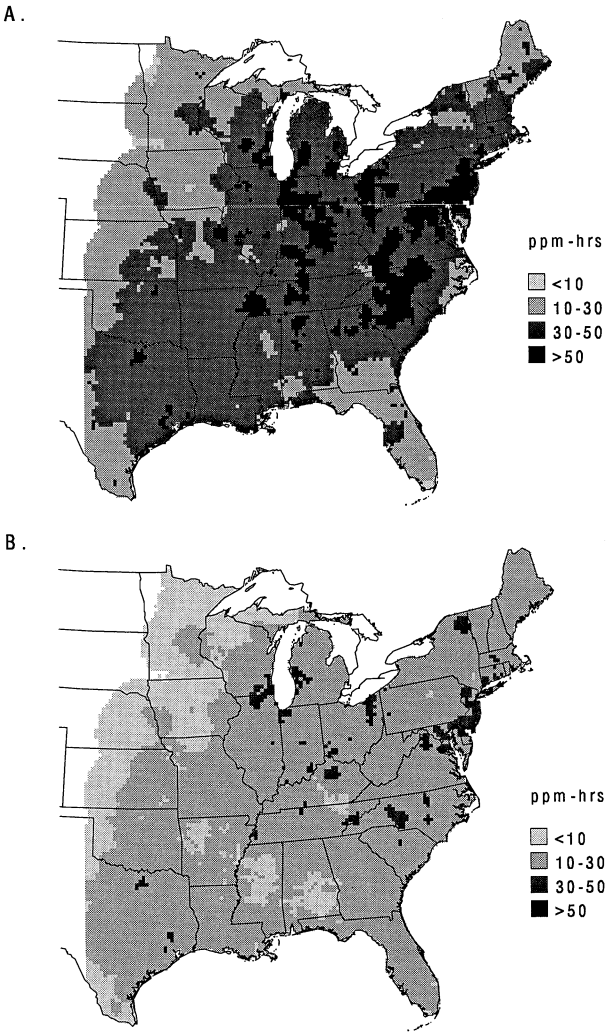

Figure 4. Estimated ozone exposure as three-month, 24-h SUM06 across the eastern United States for 1988 (**A**) and 1989 (**B**).

yields the monitored value; hence the technique honors the monitored values and the PES is ''pinned'' to the actual exposure surface at each monitored site. The PES serves to identify the trend in ozone exposure one would expect between monitored sites due to the combination of influencing factors that make up the PES. Thus, by adding information to the estimation process, the PES serves as the ''plausible model of variation'' that all interpolation techniques try to create.

The monitored values for 1988 and 1989 are used in combination with the exposure potential values for those same years to produce estimates of ozone exposure for each of the two years across the study area (Figure 4). The estimated exposure values hold true to the assumptions used in generating the surface of ozone exposure potential. That is, areas surrounding and downwind of large sources of ozone-forming precursors are predicted to have greater ozone exposure than outlying areas. This is depicted by the ozone plumes around Dallas-Fort Worth and Houston, Texas; Cincinnati, Ohio; Indianapolis, Indiana; and others. Between these major urban areas the predicted values are generally much lower. The variation between years is evident using the SUM06 indicator; 1988 was a year of much higher ozone exposure than 1989 (Figure 4). This year-to-year variation in ozone exposure will be reflected in growth response effects.

Exposure–Response Functions

A wide variety of measures have been used to describe the response of tree species to ozone exposure, including visible foliar injury, biomass partitioning, photosynthetic capacity, leaf fall. For this preliminary assessment illustrating the GIS-based approach, we have chosen change in growth as the measurement end point, and in particular, total biomass change as a function of ozone exposure. The information can come from two sources: (1) empirical data (seedling or large tree exposure studies from chambers or field) and (2) model simulations (process-based whole tree models for seedlings or large trees and stand composition models). Empirical data are statistical exposure–response models describing changes in species biomass, leaf dynamics, etc. In this preliminary assessment, we have relied exclusively on empirical data, specifically, seedling exposure–response studies.

Exposure–response functions are derived from published growth response data where possible (i.e., field exposure studies with well-characterized ozone exposures, and combinations of ozone and other stress, such as drought) (Schafer and Heagle 1989, Qui and others 1992, Karnosky and others 1995, Neufeld and others 1995) and from recently completed field exposure studies (Hogsett unpublished, Karnosky unpublished, Neufeld unpublished). The total biomass response function is expressed for each species with the Weibull model (Rawlings and Cure 1985) (Table 2). These response functions are for seedlings and are from field exposure studies conducted in open-top exposure chambers (Hogsett and others 1985). The data are limited to the conditions under which the experiments were conducted and, in a few instances, are from multiple-year exposures (loblolly pine, ponderosa pine, and Douglas fir). Unfortunately, many of the earlier published studies of tree response either did not have enough treatment levels to develop exposure–response functions or did not report the ozone exposure data necessary to calculate a SUM06 value.

Table 2. Weibull model parameters for exposure–response functions for 11 tree species as seedlings including exposure treatment and duration

Species / family	Site	Source[a]	Exposure duration (days)	Experimental SUM06 value for treatment (ppm-h)				
				1[b]	2	3	4	5
Aspen—wild	Oregon		112	0.2	16.1	72.1	102.8	
Aspen 259	Michigan	Karnosky and others (1995)	98	0.0	11.5	24.5	32.4	40.3
Aspen 271	Michigan	Karnosky and others (1995)	98	0.0	11.5	24.5	32.4	40.3
Aspen—wild	Michigan	Karnosky and others (1995)	98	0.0	11.5	24.5	32.4	40.3
Douglas fir	Oregon		234	0.1	33.4	147.2	207.2	261.5
Douglas fir	Oregon		234	0.1	33.4	147.2	207.2	261.5
Douglas fir	Oregon		230	0.1	30.4	60.6	143.0	202.9
Ponderosa pine	Oregon		230	0.1	30.4	60.6	143.0	202.9
Ponderosa pine	Oregon		280	0.9	39.2	149.4	152.6	321.8
Red alder	Oregon		118	0.0	16.0	31.8	73.4	103.6
Red alder	Oregon		112	0.1	14.5	29.1	70.1	99.9
Black cherry	Smokey Mtn Nat'l Park	Neufeld and others (1995)	76	0.0	1.9	17.1	40.6	
Black cherry	Smokey Mtn Nat'l Park	Neufeld (personal communication 1995)	140	0.0	0.0[c]	0.8	18.1	50.2
Red maple	Smokey Mtn Nat'l Park	Neufeld (personal communication 1995)	55	9.2	12.0	47.0	125.4	
Tulip poplar	Smokey Mtn Nat'l Park	Neufeld (personal communication 1995)	184	0.1	0.5	1.4	34.5	88.7
Virginia pine	Smokey Mtn Nat'l Park	Neufeld (personal communication 1995)	98	0.0	0.0[c]	1.9	21.7	51.6
Loblolly GAKR 15–19	Alabama	Qui and others (1992) Lefohn and others (1992)	555	4.9	58.5	301.5	507.0	
Loblolly GAKR 15–23	Alabama	Qui and others (1992) Lefohn and others (1992)	555	4.9	58.5	301.5	507.0	
Sugar maple	Michigan	Karnosky (personal communication 1995)	180	0.0	25.2	27.8	49.8	67.6
E. white pine	Michigan	Karnosky (personal communication 1995)	180	0.0	25.2	27.7	49.8	64.2

[a]Source of biomass and ozone exposure data for species at experimental sites other than Corvallis, Oregon.

[b]Treatment 1 is charcoal-filtered exposure.

[c]Treatment 2 is half times ambient exposure with SUM06 = 0 ppm-h.

Species Distribution

In the GIS, the study area grid surface was overlaid with a ''mask'' to block out nonrange, urban, and agricultural areas that likely do not contain a given tree species. The mask is constructed from individual species distribution maps (Little 1971) and then further delimiting the species' range using AVHRR satellite imagery identifying forested areas (Loveland and others 1991). Species density can also be included as a further delimiter of the geographic extent of the species using the forest inventory data (FIA) where available (Hansen and others 1992, Woudenberg and Farrenkopf 1995). As information becomes available, those influential environmental factors can also be included as a data layer and their influence reflected in the spatially distributed exposure–response function.

Results and Discussion

The GIS-based risk characterization approach is illustrated using seedling exposure–response biomass data for eight species of eastern forest tree species and the estimated ozone exposures for 1988 and 1989, two very different years regarding ozone exposure.

Spatial Estimates of Annual Biomass Loss

Spatial estimates of biomass loss were conducted for quaking aspen (*Populus tremuloides*), black cherry (*Prunus serotina*), tulip poplar (*Liriodendron tulipifera*), sugar maple (*Acer saccharum*), red maple (*Acer rubrum*), loblolly pine (*Pinus taeda*), virginia pine (*Pinus virginiana*), and eastern white pine (*Pinus strobus*) using estimated ozone exposure values over these species' distributions

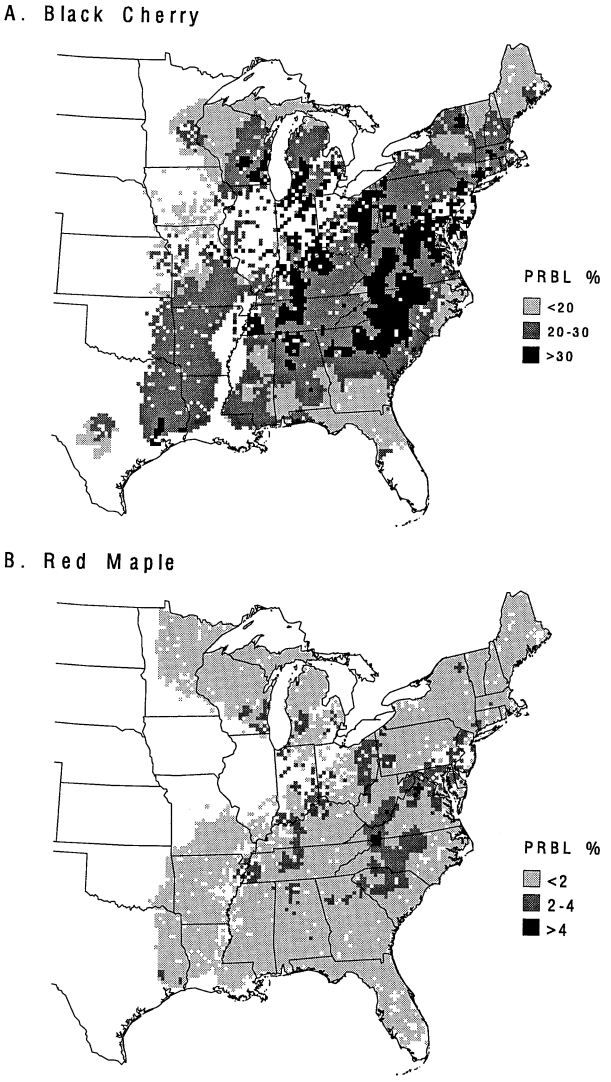

Figure 5. Map of predicted relative biomass loss (PRBL) for black cherry (**A**) and red maple (**B**) with 1988 ozone exposure. PRBL calculated for each 20-km cell based on estimated ozone exposure value (three-month SUM06) and Weibull parameters for each species' response function.

for the years 1988 and 1989. The two years are used in the assessment in order to bracket the range of response as a result of year-to-year variation in ozone exposure. The year 1988 represents the highest ozone exposure year in the decade of the 1980s, and 1989 represents a lower than average year of exposure (Lee and others 1994).

Maps of the spatial distribution of biomass loss for each species were generated using the GIS. The maps indicate the relative spatial risk each species is subject to based on the spatial distribution of ozone exposure. Selected maps are shown to illustrate the range of response among the species considered and the variation in response within a species with genotype and exposure year (Figures 5–8 below). These are obvious sources of growth response variation, but serve to place some initial bounds in this preliminary characterization. Relative predicted total biomass loss (RPBL) was calculated for each 20-km cell in the study area using two input parameters: (1) the estimated three-month SUM06 exposure value for each 20-km cell for the years 1988 and 1989 (Figure 4), and (2) the exposure–response Weibull model parameters for each species (Table 2). The additional three species (ponderosa pine, Douglas fir, and red alder) in Table 2 are all western forest species and are included for comparability with the eastern tree species used in this illustration of the risk characterization approach.

The relative predicted biomass losses based on the seedling-derived exposure–response functions ranged from 0 to greater than 35% per year (Table 2). The range of response between species is dramatic (Figure 5). Black cherry and red maple have approximately the same range across most of the eastern United States, and both are present in most forest types; however, neither is the dominant species in any forest type. Both species have the same growth strategy, but black cherry is predicted from seedling growth response functions to exhibit annual losses in total biomass of greater than 20% over almost all of its range with 1988 exposure values (Figure 5A), whereas red maple is predicted to have annual losses of less than 2% over the same range and exposure (Figure 5B). The spatial variation in response for two pine species, eastern white pine and loblolly pine is shown in Figure 6. Loblolly pine is predicted to have less than 3%–6% loss annually over 80% of its range (Figure 6A). Eastern white pine, on the other hand, has more response variation across its range (Figure 6B). It may experience greater than 15% annual losses under 1988 exposure levels in small localized areas through western Pennsylvania, eastern Ohio, and down through the Appalachian Mountains (less than 10% of the species coverage), but biomass losses $<$10% are predicted for more than 50% of its area. For all species there were localized areas in its range that would be predicted to have relatively greater losses and risk.

The variation in biomass loss as a function of year-to-year ozone exposure is shown in Figure 7 with growth-response data of a wild population of aspen seedlings as an example. The biomass losses are substantially greater across the species distribution during 1988 compared to 1989 (Figure 7). For black cherry, total biomass losses of greater than 30% are predicted for more than 90% of its area in 1988 (Figure 5A), whereas with 1989 exposures

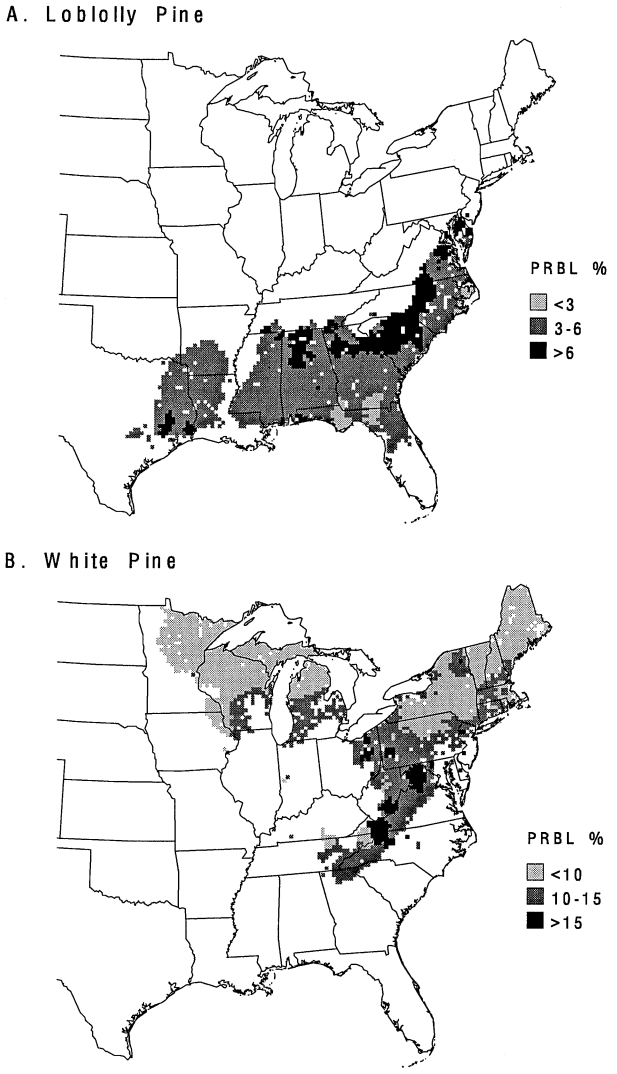

Figure 6. Map of predicted relative biomass loss (PRBL) for loblolly pine (**A**) and eastern white pine (**B**) with 1988 ozone exposures. PRBL calculated for each 20-km cell based on estimated ozone exposure value (three-month SUM06) and Weibull parameters for each species' response function.

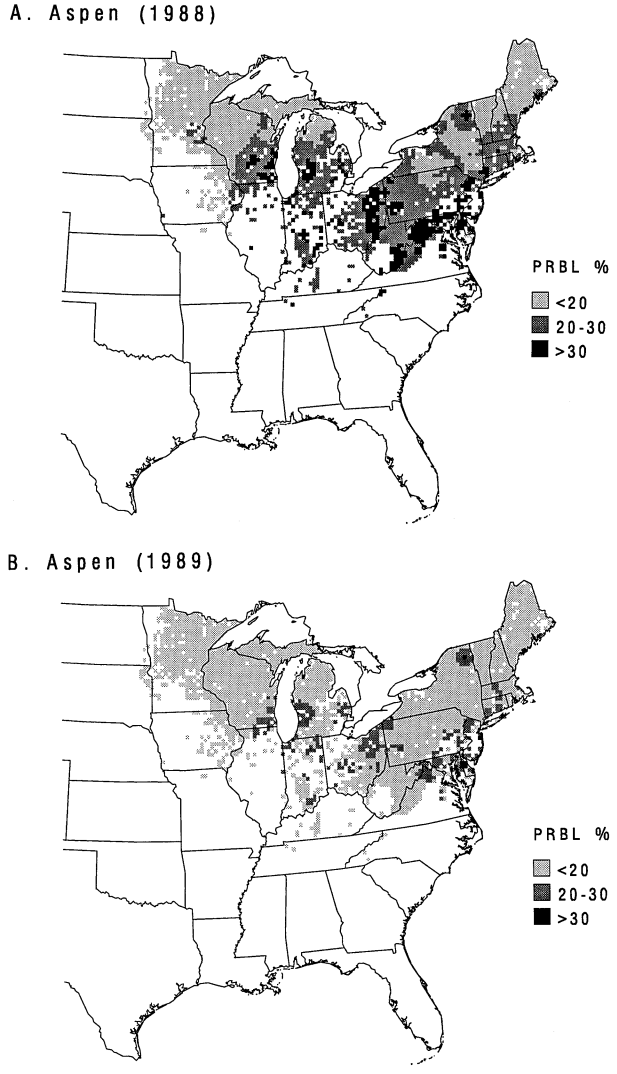

Figure 7. Variation in aspen seedling biomass loss with year-to-year exposure variation: 1988 (**A**) and 1989 (**B**) estimated exposures. PRBL calculated for each 20-km cell based on estimated ozone exposure value (three-month SUM06) and Weibull parameters for each species' response function.

less than 10% of its distribution is predicted to have biomass losses of even 20% (map not shown).

The variation in the response due to genotypic differences is illustrated in Figure 8 with two different clones of quaking aspen from Michigan having different sensitivities to ozone (Karnosky and others 1995). The biomass loss in the sensitive clone 259 (Figure 8A) is dramatically greater across the species distribution than a relatively insensitive clone 271 (Figure 8B).

Variation in growth response to ozone exposure can result from different climates and growing environments (e.g., drought, nutrient level), pest/pathogen interactions, exposure intensity and dynamics, and genetics (Hogsett and others 1988). Presently, there are no empirical data to quantify the alteration in growth response as a function of these influential factors. Later risk characterizations using these same GIS-based techniques and process-based model simulations will be able to refine these losses and their spatial distribution as a function of growing environment, genetics, or particular temporal distributions of ozone concentrations typical of certain forested areas.

Area-Weighted Total Biomass Loss

The area-weighted annual predicted total biomass losses for the eight eastern US forest species as seedlings for 1988 and 1989 are shown in Figure 9 with percentile

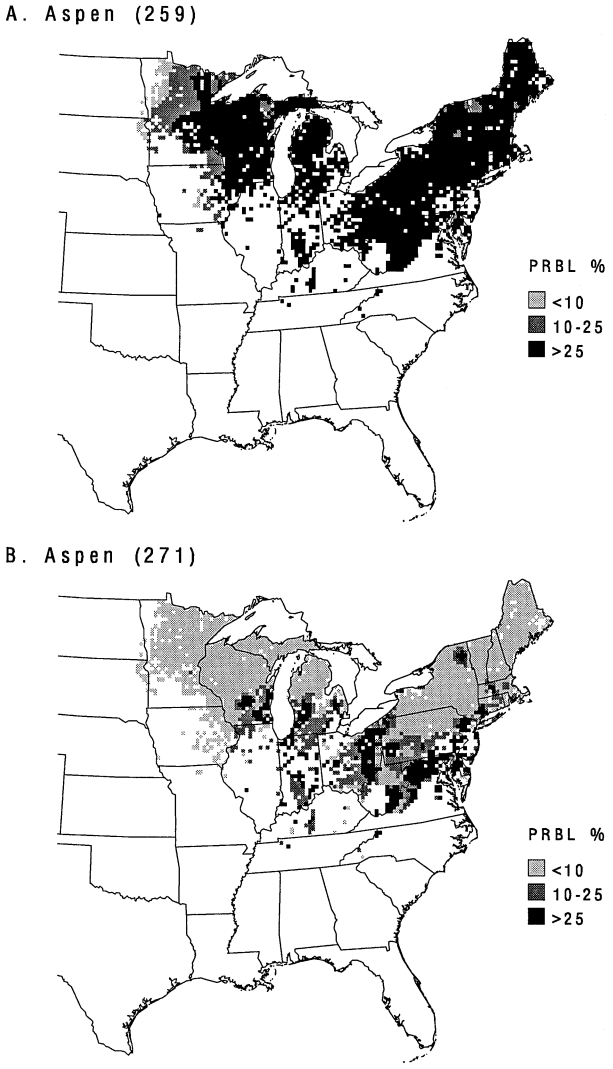

Figure 8. Variation in aspen seedling biomass loss with genotype with estimated 1988 ozone exposure. Clone 259 (**A**) and clone 271 (**B**) (Karnosky and others 1995). PRBL calculated for each 20-km cell based on estimated ozone exposure value (three-month SUM06) and Weibull parameters for each species response function.

distributions of the response included in a box plot. A predicted biomass loss is taken from each 20-km cell in the species' seedling total biomass loss maps, those values are weighted for area, and the distribution is plotted showing the 10th, 25th, 50th, 75th, and 90th percentiles, indicating the percent loss in biomass for 10%, 25%, 50%, 75%, and 90% of that species' area. The range in the response is different between species. For example, the relatively small range of predicted biomass loss of loblolly pine (4%–7%) across all its area (10th–90th percentiles) compared to sugar maple (0%–60%) across all its range. The biomass loss for 50% of the species' distribution (50th percentile, Figure 9) range from 0% for Virginia pine and red maple to 33% for the sensitive aspen clone 259. Based on the median value for each species, the relative sensitivity would fall into three groups based on area-weighted annual biomass loss in seedlings to estimated 1988 exposures (Figure 9A): (1) sensitive—aspen and black cherry with annual losses ranging from 14% to 33%; (2) moderately sensitive—tulip poplar, loblolly pine, eastern white pine, and sugar maple having annual losses of 5%–13%, and (3) insensitive—Virginia pine and red maple, which exhibited annual losses of 0%–1%. Biomass losses for each of the species predicted for 1989 were significantly less (Figure 9B).

Predicted Relative Biomass Loss in Tree Seedlings and Comparison to Crop Yield Losses

A comparison of relative predicted biomass loss (RPBL) at a given level of exposure is a first approximation of ranking a species' sensitivity to ozone. Table 3 lists 20 studies and 11 species of trees giving their predicted relative loss in total biomass at three selected three-month, 24-h SUM06 values. These particular SUM06 values (16.5, 26.4, and 39.7 ppm-h) were determined from the percentile distributions of average predicted relative crop yield losses of all crops (Lee and others 1994). A three-month SUM06 of 26.4 ppm-h is the concentration level that would protect 50% of the crops from yield losses greater than 10%. The total annual biomass losses with a three-month SUM06 of 26.4 ppm-h is predicted to range from 0% in Douglas fir (Hogsett unpublished) to 25% in aspen clone 259 (Karnosky and others 1995) (Table 3). As with the ranking suggested by the area-weighted median (50th percentile) predicted total biomass losses (Figure 9), the annual biomass losses at 26.4 ppm-h were high in aspen (10%–25%) and black cherry (16%–21%) relative to losses of 3%–9% in ponderosa pine, red alder, tulip poplar, and eastern white pine, and losses of less than 4% in loblolly pine, Virginia pine, Douglas fir, and sugar maple.

Another type of comparison is possible using an average predicted relative total biomass loss for all tree seedlings (Table 2; 11 species) in this assessment (Figure 10). A similar average predicted relative yield loss function and distribution was produced for all crops in the National Crop Loss Assessment Program (NCLAN) (Tingey and others 1991, Lee and others 1994). This averaging of exposure–response across all species is a means to predict the degree of protection afforded at various concentration levels of ozone. At 20 ppm-h, 4% losses in total biomass would be predicted annually in 50% of the tree species studied based on seedling

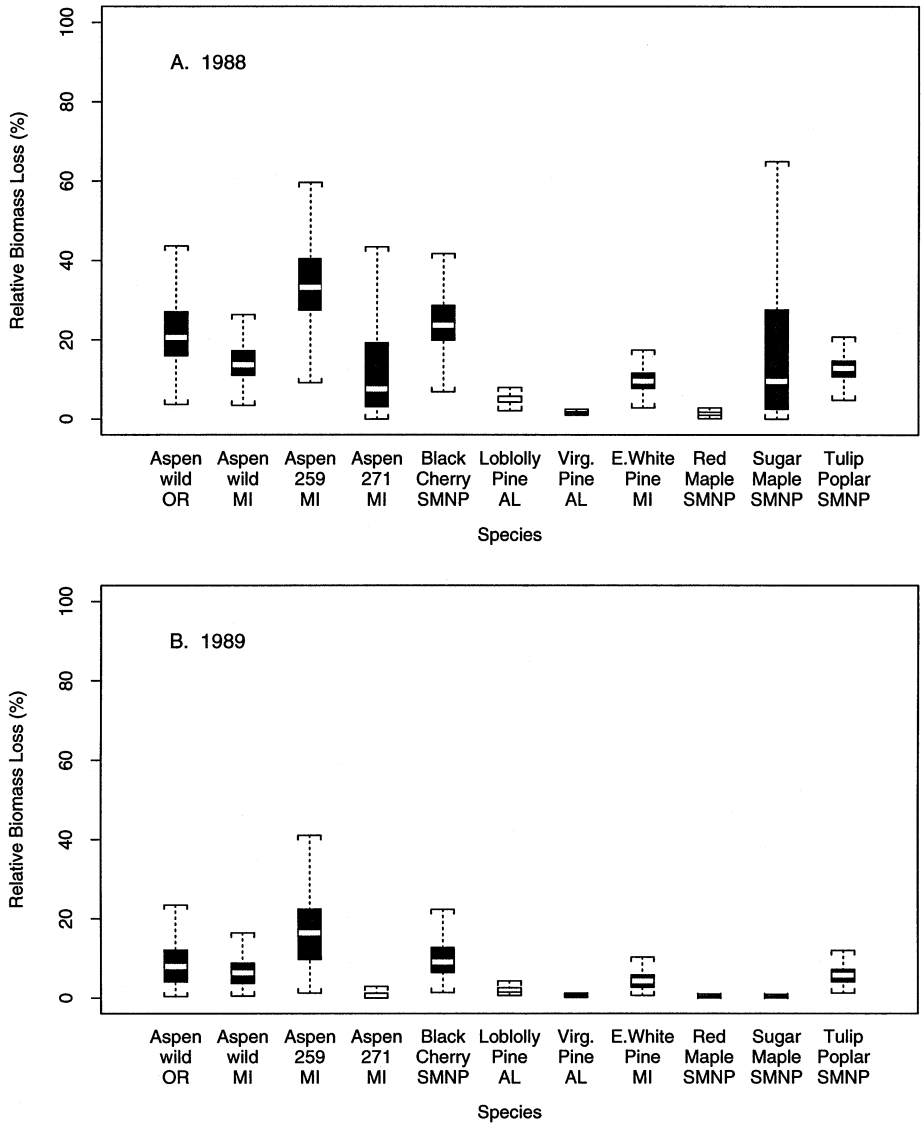

Figure 9. Box plots of annual area-weighted predicted relative biomass loss for the eight tree species with estimated 1988 (**A**) and 1989 (**B**) ozone exposure. The predicted biomass loss is taken from each 20-km cell in the species' distribution, weighted for area, and the distribution plotted showing 10th (bracket), 25th (lower shaded box), 50th (clear bar in shaded box), 75th (upper shaded box), and 90th (bracket) percentiles. The percentiles represent the area of the species exhibiting that level or less of biomass loss. OR = Oregon site, MI = Michigan site, SMNP = Smoky Mt. National Park, AL = Alabama.

response (Figure 10). This is a small number, but as an annual loss in total biomass of a seedling it could be a significant factor in seedling survival, forest regeneration, or reforestation (Kormanik 1986). A large portion of the eastern United States is experiencing three-month SUM06 of greater than 20 ppm-h (Figure 4). Annual biomass losses of 10% are predicted in tree seedlings at three-month SUM06 values of 37 ppm-h (Figure 10). In comparison, a SUM06 value of 39.7 ppm-h is predicted to protect 75% of the crops from 10% loss in yield (Lee and others 1994).

Future Risk Characterization

Future risk characterizations are planned using the same GIS-based approach (Figure 1), but including future additions of empirical exposure–response functions of species, process-based model simulations to

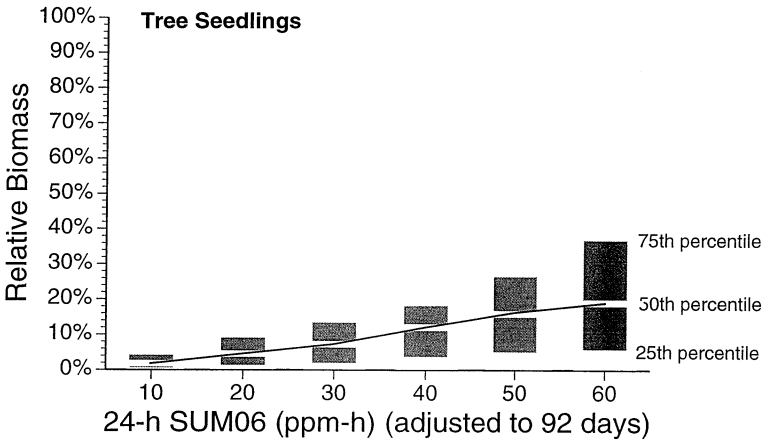

Figure 10. Average predicted relative biomass loss from 26 tree seedling studies (Table 2). Separate regressions were calculated for studies with multiple harvests and/or cultivars resulting in a total of 56 equations from the 26 seedling studies. Each equation was used to calculate the predicted relative yield or biomass loss at three-month, 24-h SUM06 exposure values of 10, 20, 30, 40, 50, and 60 ppm-h and the distributions of the resulting losses plotted. The solid line is the calculated Weibull fit at the 50th percentile.

Table 3. Predicted annual biomass loss at selected 92 day SUM06 values

	Predicted annual biomass loss (%) as a function of SUM06 adj. to 92 days (ppm-h/yr) =		
Species/family	16.5[a]	26.4[b]	37.7[c]
Aspen—wild	8	14	23
Aspen 259	17	25	36
Aspen 271	0	2	11
Aspen—wild	6	10	15
Douglas fir	0	0	0
Douglas fir	1	2	3
Douglas fir	0	0	0
Ponderosa pine	5	8	14
Ponderosa pine	1	3	6
Red alder	4	7	10
Red alder	5	9	14
Black cherry	13	21	31
Black cherry	10	16	25
Red maple	0	1	1
Tulip poplar	5	8	12
Loblolly, GAKR 15–91	2	4	5
Loblolly, GAKR 15–23	1	1	2
Sugar maple	0	1	12
E. white pine	4	7	10
Virginia pine	1	1	1

[a]16.5 ppm-h is the level needed to protect against 10% yield loss for 75% of crops (Tingey and others, 1991).

[b]26.4 ppm-h is the level needed to protect against 10% yield loss for 50% of crops (Tingey and others, 1991).

[c]39.7 ppm-h is the level needed to protect against 20% yield loss for 50% of crops (Tingey and others, 1991).

account for long-term effects, age/size influence, and environmental factors. Figure 11 illustrates the combination of these elements in the GIS.

The determination and quantification of long-term effects of ozone are not easily accomplished via experimental manipulation. To describe these effects, model simulations at two levels of complexity—a single tree and mixed-stand response through time are used.

The growth response simulation of a single tree will rely on TREGRO, a physiologically based growth model (Laurence and others 1993, Weinstein and others 1991), parameterized from experimental data. TREGRO provides a carbon, water, and nutrient balance for the simulated tree over some time period. In the case of response functions generated from TREGRO for future risk characterizations (Figure 11), a series of multiple-year (three- to five-year) simulations will be conducted using four to five ozone scenarios, encompassing the range of estimated ozone exposure from regions relevant to the species, and climate data from across the species' region (three sites) to generate response functions that include the influence of spatially distributed environmental and exposure factors. The question of multiple environmental factor exposure–response functions is a particularly important one. Since the objective of the assessment is to provide an integration of the likely response of a tree or forest type to ozone over its range, the modification of response by other environmental and biological factors must be addressed. Most experiments are conducted under conditions that are conducive for plant growth and response to ozone. It has been widely reported that the response of a tree to ozone may be altered by drought, soil fertility, or temperature, as well as other factors (US EPA 1986, Hogsett and others 1988). Additionally, the genotype of the tree is important in determining its response to ozone (Roose 1991), but this is only rarely assessed. Simulations offer the opportunity to assess the likely importance of these interactions with ozone. For instance, a series of simulations may be conducted applying hypothetical sensitivities to the species under examination. While the exact response of various genotypes may not be known, bounds may be placed on the

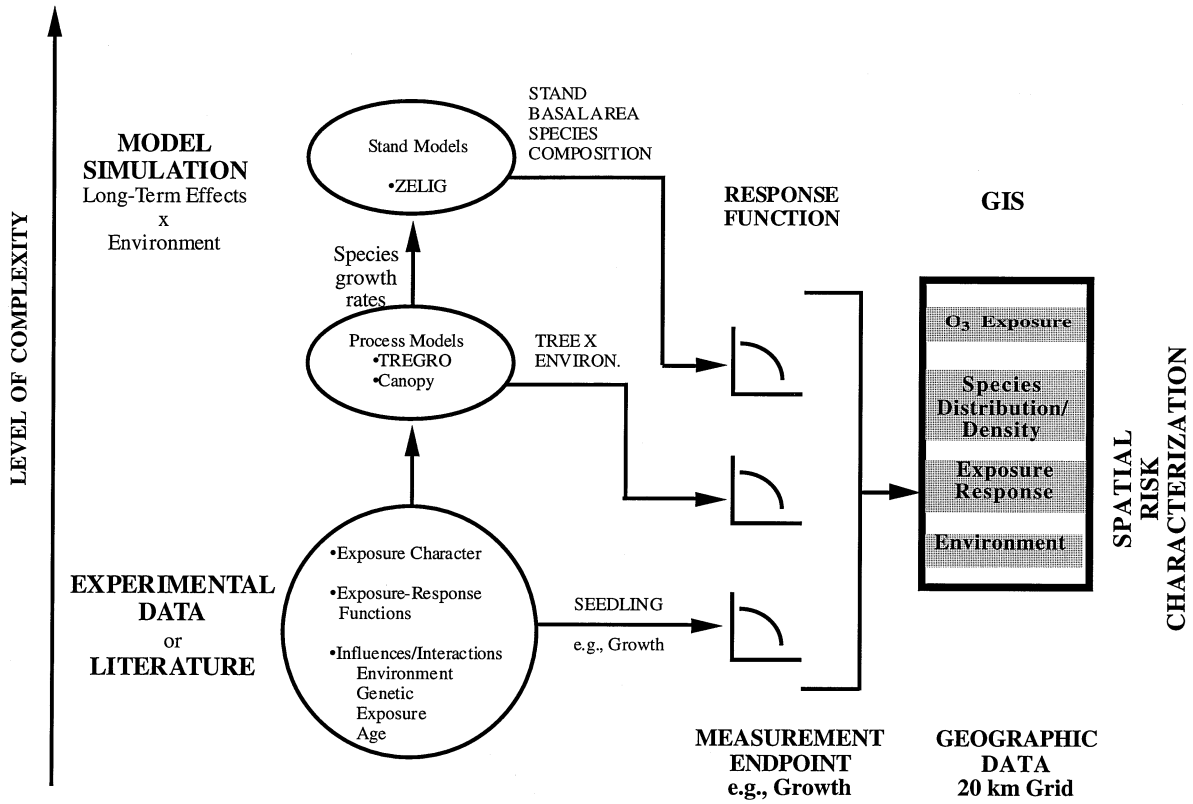

Figure 11. GIS-based integrated risk characterization. The flow diagram illustrates the connections between experimental data and model simulations of large tree and stand growth responses with relevant environmental interactions; derived exposure–response functions for seedlings, trees, and stands; and how the response functions are integrated in the GIS as data layers with ozone exposure estimations, species distributions, and local influential environmental factors to give a spatial risk characterization of ozone impact on forests at the seedling, large tree, individual, or stand level.

expected response. Model simulations will allow us to reduce the uncertainty and place bounds on the response across the species' range. The growth response or changes in biomass of a single tree species will be passed to the GIS to produce a spatial model of a species' growth over time (Figure 11).

Simulated growth rates of individual species to several ozone exposure regimes and various environmental scenarios from TREGRO will be passed to ZELIG, a forest stand simulator (Urban 1990). Results of the exposure–response simulations in TREGRO are used to generate three variables: total tree growth rate, leaf area, and root/shoot ratio. These variables are passed to ZELIG, where they are used to modify parameters in simulations of stand growth and development. The response outputs from this model will be basal area of competing species within a stand, e.g., white fir and ponderosa pine, indicating the species composition of the stand exposed to ozone in that simulated growing environment. Stand simulations will be run for extended time periods (50–100 years) to characterize changes in stand composition based on species sensitivity to ozone. Finally, the results from ZELIG will be incorporated into the GIS analysis to produce a spatial model of forest species response to ozone (Figure 1).

Uncertainty in Risk Characterization

There are uncertainties attached to each component involved in the derivation of the risk characterization. In this preliminary spatial risk characterization, there is uncertainty associated with: (1) estimation of exposure in non-monitored areas, (2) climate and meteorology data, (3) species distribution, and (4) experimentally derived exposure–response functions for seedlings. Biomass loss for each species in this preliminary assessment has been predicted using seedling-derived growth response functions, and there is an unknown error associated with seedling versus large tree response to ozone. Current research is addressing this uncertainty. In the planned future assessments of long-term effects, there will be uncertainty associated with the model

simulations. In the integration of these data and model simulations in the GIS, there is the error associated with the combination of these components. For instance, in using literature-based exposure–response functions, the error associated with the experiment, the sampling, and the analysis must be recognized. Further, when these responses are scaled up for future use in a tree (TREGRO) or a stand model (ZELIG), the uncertainty must be carried along, and, in fact, expands considerably due to the variations of weather and other factors that determine tree growth. Thus, in the stand simulation, an examination must be made of the range of stands that might result from the error associated with the postulated exposure–response, as well as the variation in stand that results from stochastic processes within the stand model itself. Specific examples of uncertainties that must be considered include the parameterization of TREGRO and ZELIG, including responses of trees to ozone, water, and nutrients; root/shoot allocation patterns; and species sensitivity to environmental conditions. As the results are passed to the GIS, associated errors must again be recognized. Species distributions, temperature, ozone, and other environmental conditions are estimates and have an associated error that must be recognized in the spatial model. With TREGRO and ZELIG, we will examine uncertainty through sensitivity analysis of the parameters, as well as by conducting model runs under enough conditions to place bounds on the error. For example, if we take care to generate responses that include those predicted to occur at levels far above or below those that might normally be expected to occur, we may judge the sensitivity of the estimate we are producing and at least recognize if an error is likely to have a large effect. Uncertainty associated with expression of exposure–response as ambient exposure rather than concentration taken up by canopy (i.e., dose) will also be considered in these simulations.

A source of error that can be propagated through the entire assessment is in the estimation of ozone exposure in forested areas since the exposure–response models require these estimates. As previously stated, less than 2% of all ozone monitoring sites are located in forested areas; hence exposures in forests must be estimated, and using traditional interpolation to make these estimates over forests is highly questionable. While our approach does give results that are intuitively more appealing than traditional interpolation techniques, and still consistent with known values, there is no means by which to estimate the certainty of the prediction in nonmonitored forests. In estimating exposure values there were three components: (1) the actual monitoring site values for a given year, e.g., 1988; (2) monthly NO_x emisions from annual inventory data for 1985; and (3) meterological data. All three components have some degree of uncertainty associated with them. The precursor emissions and meteorological data have perhaps a greater degree of uncertainty than the monitoring sites. The accuracy of emission inventory data has been questioned (National Research Council 1991), but without quantification of this uncertainty we have chosen to use this source as ''best available'' data in this assessment. The meteorological data had different temporal scales, e.g., monthly averages for 1985 (solar radiation) and long-term averages of 30 years (wind direction), but this does not necessarily introduce any quantifiable level of uncertainty in the estimate. These data do reflect typical conditions and interregional trends, and thus reflect the meterorlogical conditions that affect ozone formation and transport. Month- and year-specific meterological data would presumably improve the exposure potential surface; however, the data are not available and if they were, the computer time and costs for generating these monthly surfaces might not be justified with only the slight changes in the predicted values from such data.

Aside from the accuracy of the exposure–response estimates and calculations, map interpretation can be a major source of error in perception. Maps depicting biomass reduction for the individual tree species imply a homogeneously dense monoculture forest. Our maps of species range do not reflect where a particular species is key ecologically, e.g., dominant or codominant, or where a particular species is economically important to the region. The AVHRR satellite data were used to mask out urban and agricultural areas but other factors potentially influence the presence/absence of a species within the range defined by Little (1971). These include islands of high elevation that might not be conducive to that particular species or commercial monoculture tree plantations of a different species. These problems could be ameliorated by using large-scale forest stand maps or finer-scale satellite classification. Future assessments will incorporate forest inventory assessment (FIA) data to account for county-level species density to further delimit species distribution (Hansen and others 1992, Woudenbergand Farrenkopf 1995).

Conclusions

Even with the uncertainties, this preliminary assessment has indicated the usefulness of and potential for a spatial approach to assessing the extent and magnitude of the risk that tropospheric ozone presents to the forested areas of the eastern United States based on

current estimated ozone concentrations. The maps provide a visual record of the variation in productivity of a number of species as a result of the variation in ambient ozone exposures estimated to occur in forested areas. The integration of exposure–response functions allows the estimation of the magnitude of the effect on biomass and estimatation of the extent of the effect across the species' range. Both the maps and the empirical data on magnitude and extent of effects provide a means to assess priorities for concern of impact and future data needs. The GIS-based approach has the capacity to include, as it becomes available, those spatial factors influencing ozone response, e.g., water availability, nutrient levels, soil types, etc., as well as including model simulations of response at the individual level or stand level incorporating these spatial environmental and exposure influences and also the mechanistic basis for the effect of age and size in the response.

In particular, this preliminary assessment of the extent and magnitude of the effect of ozone on tree species in the eastern United States indicated a wide range of annual biomass loss with estimated ambient ozone for each species' range. Annual biomass losses ranged from 0%–33%, depending on species and concentration of ozone across the range of the species. The two most sensitive species were black cherry and aspen with greater than 20% total biomass loss predicted over greater than 50% of the species range. These are substantial losses on an annual basis. Four of the eight species considered (tulip poplar, loblolly pine, sugar maple, and eastern white pine) were predicted to have 5%–12% annual biomass loss and have a large portion of their individual ranges experiencing these losses. For example, eastern white pine has biomass losses of 5%–10% predicted to occur on greater than 50% of its range.

Based on the estimations of this assessment, it would also appear that substantial annual biomass losses (10%–21%) would still be occurring in black cherry and aspen at the ozone concentration level considered to prevent 10% crop yield loss in 50% of the crops (three-month SUM06 of 26.4 ppm-h). The four moderately sensitive species would be predicted to experience annual losses of 1%–9%, and less than 1% in Virginia pine and red maple. The relative sensitivities are similar to previous seedling studies of some of these same species, even though the study may not have specifically developed total biomass exposure response (Kress and Skelly 1982, Reich and Amundson 1988).

These estimations of ozone impact may be high and may be reduced when consideration of age and size is incorporated into the estimation, as well as consideration of local environmental factors, but this assessment does give an indication of the potential spatial impact with current ambient ozone levels in this region, and the approach offers a means to illustrate the extent of the risk through spatially distributed exposure–response functions.

Literature Cited

EarthInfo, Inc. 1992a. EarthInfo's national climatic data center surface airways user's manual. Boulder, Colorado.

EarthInfo, Inc. 1992b. EarthInfo's national climatic data center summary of the day user's manual. Boulder, Colorado.

Eyre, F. H. 1980. Forest cover types of the United States and Canada. Society of American Foresters, Washington, DC.

Hansen, M. H., Frieswyk, T., Glover, J. F., and J. F. Kelly. 1992. The Eastwide forest inventory data base: Users manual. Gen. Tech. Rep. NC-151. USDA, Forest Service, North Central Forest Experiment Station, St. Paul, Minnesota, 48 pp.

Hogsett, W. E., and A. A. Herstrom. 1991. GIS-based risk assessment: Applications from an approach to ozone risk assessment. Pages 36–43 *in* Plant tier testing: A workshop to evaluate non-target plant testing in subdivion J pesticide guidelines. EPA/600/9-91/041, US EPA, Washington, DC.

Hogsett, W. E., D. T. Tingey, and S. R. Holman. 1985. A programmable exposure control system for determination of the effects of pollutant exposure regimes on plant growth. *Atmospheric Environment* 19:1135–1145.

Hogsett, W. E., D. T. Tingey, and E. H. Lee. 1988. Ozone exposure indices: Concepts for development and evaluation of their use. Pages 107–138 *in* W. W. Heck, O. C. Taylor, and D. T. Tingey (eds.), Assessment of crop loss from air pollutants: Proceedings of an international conference. Elsevier Applied Science, London.

Karnosky, D., Z. E. Gagnon, R. E. Dickson, M. D. Coleman, E. H. Lee, and J. G. Isebrands. 1995. Changes in growth, leaf abscission and biomass associated with seasonal ozone exposures of *Populus tremuloides* clones and seedlings. *Canadian Journal of Forest Research* (in press).

Kormanik, P. P. 1986. Lateral root morphology as an expression of sweetgum seedling quality. *Forest Science* 32(3):595–604.

Kress, L. W., and J. M. Skelly. 1982. Response of several eastern forest tree species to chronic doses of ozone and nitrogen dioxide. *Plant Disease* 66:1149–1152 (erratum 67:233).

Laurence, J. A., R. J. Kohut, and R. G. Amundson. 1993. Use of TREGRO to simulate the effects of ozone on the growth of red spruce seedlings. *Forest Science* (in press).

Lee, E. H., D. T. Tingey, and W. E. Hogsett. 1988. Evaluation of ozone exposure indices in exposure-response modeling. *Environmental Pollution* 53:43–62.

Lee, E. H., W. E. Hogsett, and D. T. Tingey. 1994. Attainment and effects issues regarding alternative secondary ozone air quality standards. *Journal of Environmental Quality* 23(6):1129–1140.

Lefohn, A. S., and A. A. Lucier. 1991. Spatial and temporal variability of ozone exposure in forested areas of the USA

and Canada. *Journal of the Air Pollution Control Association* 41:694–701.

Lefohn, A. S., H. P. Knudsen, J. A. Logan, J. Simpson, and C. Bhumralkar. 1987. An evaluation of the kriging method to predict 7-h seasonal mean ozone concentrations for estimating crop losses. *Journal of the Air Pollution Control Association* 37:595–602.

Lefohn, A. S., D. S. Shadwick, M. C. Somerville, A. H. Chappelka, B. G. Lockaby, and R. S. Meldahl. 1992. The characterization and comparison of ozone exposure indices used in assessing the response of loblolly pine to ozone. *Atmospheric Environment* 26A:287–298.

Little, E. L., Jr. 1971. Atlas of United States trees. Miscellaneous Publication No. 1146. US Department of Agriculture, Forest Service, Washington, DC.

Logan, J. A. 1988. The ozone problem in rural areas of the United States. Pages 327–344 *in* I. S. A. Isaksen (ed.), Tropospheric ozone. D. Reidel Publishing, Dordrecht.

Loveland, T. R., J. W. Merchant, D. O. Ohlen, and J. F. Brown. 1991. Development of a land-cover characteristics database for the conterminous US. *Photogrametric Engineering and Remote Sensing* 75(11):1453–1463.

Miller, P. R., S. R. McBride, S. L. Schilling, and A. P. Gomez. 1989. Trend of ozone damage to conifer forests between 1974 and 1988 in the San Bernardino Mountains of Southern California. Pages 309–324 *in* R. K. Olson and A. S. Lefohn (eds.), Effect of air pollution on western forests. Transactions Series. Air and Waste Management Association, Pittsburg.

Musselman, R. C., P. M. McCool, and A. S. Lefohn. 1994. Ozone descriptors for an air quality standard to protect vegetation. *Journal of Air and Waste Management* 44:1383–1390.

National Research Council. 1991. Rethinking the ozone problem in urban and regional air pollution. National Academy Press, Washington, DC, 489 pp.

Neufeld, H. S., E. H. Lee, J. R. Renfro, W. D. Hacker, and B.-H. Yu. 1995. Sensitivity of seedlings of black cherry (*Prunus serotina* Ehrh.) to ozone in Great Smoky Mountains National Park: 1. Exposure–response curves for biomass. *New Phytologist* 130:447–459.

Oliver, M. A. 1990. Kriging: A method for interpolation for geographical information systems. *International Journal of Geographical Information Systems* 4:313–332.

Pinkerton, J. E., and A. S. Lefohn. 1987. The characterization of ozone data for sites located in forested areas of the eastern United States. *Journal of the Air Pollution Control Association* 37:1005–1010.

Pye, J. M. 1988. Impact of ozone on the growth and yield of trees: A review. *Journal of Environmental Quality* 17:347–360.

Qiu, Z., A. H. Chappelka, G. L. Somers, B. G. Lockaby, and R. S. Meldahl. 1992. Effects of ozone and simulated acidic precipitation on above- and below-ground growth of loblolly pine (*Pinus taeda*). *Canadian Journal of Forest Research* 22:582–587.

Rawlings, J. O., and W. W. Cure. 1985. The Weibull function as a dose-response model to describe ozone effects on crop yields. *Crop Science* 25:807–814.

Reich, P. B., and R. G. Amundson. 1985. Ambient levels of ozone reduce net photosynthesis in tree and crop species. *Science* 230:566–570.

Roose, M. L. 1991. Genetics of response to atmospheric pollutants. Pages 111–126 *in* G. E. Taylor, L. F. Pitelka, and M. T. Clegg (eds.), Ecological genetics and air pollution. Springer-Verlag, New York.

Schafer, S. R., and A. S. Heagle. 1989. Growth responses of field-grown loblolly pine to chronic doses of ozone during multiple growing seasons. *Canadian Journal of Forest Research* 19:821–831.

Suter, G. W. 1990. End points for regional ecological risk assessments. *Environmental Management* 14:9–23.

Tingey, D. T., W. E. Hogsett, and S. Henderson. 1990. Definition of adverse effects for the purpose of establishing secondard national ambient air quality standards. *Journal of Environmental Quality* 19:635–639.

Tingey, D. T., W. E. Hogsett, E. H. Lee, A. A. Herstrom, and S. H. Azevedo. 1991. An evaluation of variou alternaitve ambient ozone standards based on crop yield loss data. Pages 272–288 *in* R. L. Berglund, D. R. Lawson and D. J. McKee (eds.), Transactions: Tropospheric ozone and the environment. Air and Waste Management Association, Pittsburgh.

Urban, D. L. 1990. A versatile model to simulate forest pattern. A user's guide to ZELIG version 1.0. Environmental Sciences Department, The University of Virginia, Charlottesville.

US Department of Commerce. 1992. 1990 Census of population and housing summary tape file 1C. Bureau of Census, Data User Services Division, Washington, DC.

US EPA (US Environmental Protection Agency). 1986. Air quality criteria for ozone and other photochemical oxidants, Vol III. EPA-600/8-84-020cF. Washington, DC.

US EPA (US Environmental Protection Agency). 1992a. Framework for ecological risk assessment. EPA/630/R-92/001. Washington, DC.

US EPA (US Environmental Protection Agency). 1992b. National air pollutant emissions estimates, 1900–1991. EPA-454/R-92-013. Office of Air Quality Planning and Standards, Research Triangle Park, North Carolina.

Watson, D. F., and G. M. Phillip. 1985. A refinement of inverse distance weighted interpolation. *Geo-Processing* 2:315–327.

Weinstein, D. A., R. M. Beloin, and R. D. Yanai. 1991. Modeling changes in red spruce carbon balance and allocation in response to interacting ozone and nutrient stresses. *Tree Physiology* 9:127–146.

Wolff, G. T., P. J. Lioy, and R. S. Taylor. 1987. The diurnal variations of ozone at different altitudes on a rural mountain in the eastern United States. *Journal of the Air Pollution Control Association* 37:45–48.

Woudenberg, S. W., and T. O. Farrenkopf. 1995. The Westwide forest inventory data base: User's manual. Gen. Tech. Rep. INT-GTR-317. US Department of Agriculture, Forest Service, Intermountain Research Station, Ogden, Utah, 67 pp.